Geophysical Research Letters

RESEARCH LETTER
10.1029/2024GL112514

Glacier Surges and Seasonal Speedups Integrated Into a Single, Enthalpy-Based Model Framework

Y. Terleth[1], T. C. Bartholomaus[1], E. Enderlin[2], T. D. Mikesell[3], and J. Liu[2]

[1]Department of Earth and Spatial Sciences, University of Idaho, Moscow, ID, USA, [2]Cryosphere Remote Sensing and Geophysics (CryoGARS) Laboratory, Department of Geosciences, Boise State University, Boise, ID, USA, [3]Norwegian Geotechnical Institute (NGI), Oslo, Norway

Abstract Glacier speedups occur on daily to centennial timescales. While basal water and subglacial drainage configuration are thought to drive glacier speedups across these timescales, it remains unclear whether this forcing always occurs through the same mechanisms. Here, we explore whether the enthalpy model of glacier surging can explain speedups over a broader range of timescales if modified to account for seasonality in surface melt and continuous water supply to the glacier bed. We simulate velocity oscillations that range from seasonal to >100 years. Our model results more closely resemble observations of surges than previous model versions because ice flow variability at seasonal and multi-year timescales is reproduced simultaneously through hydrological forcing. Under favorable conditions, seasonal water delivery to the bed gradually accumulates in a poorly-connected basal drainage system, priming the glacier to surge. Surges themselves are marked by high water fluxes and enthalpy drainage from the glacier base.

Plain Language Summary Glacier speeds vary over time periods ranging from hours to centuries. Liquid water present at the base of glaciers affects ice speed but it is unclear whether the links between liquid water and ice speed are the same across all timescales. Recent efforts to model multi-year cycles of fast glacier flow, known as glacier surges, show that a gradual build-up of heat and/or water at the base of glaciers could drive ice flow instabilities. However, this modeling approach has thus far not accounted for seasonal variations in water flux through glaciers and their influence on glacier flow. In this work we implement seasonal variability in air temperatures within an existing model of glacier surges. We explore the effects of changing the water supply to the glacier base, finding that glaciers that do not transmit surface water through the glacier easily are more prone to surging and that glaciers with a poorly connected drainage system at their base might be more likely to surge. The simulation of surges here demonstrate that a single set of physical relationships between water within glaciers and glacier motion can reproduce a spectrum of observed behaviors, without the need for invoking more complicated physics.

Key Points:

- An enthalpy model is used to simulate realistic variability in glacier velocities, simultaneously over seasonal to multi-year timescales
- Enthalpy modeling can simulate realistic surges, but only under low water supply to the bed and low basal hydraulic transmissivity
- Modeling suggests that poor drainage primes the glacier to surge, but the surge itself is marked by improved basal water flow

Supporting Information:

Supporting Information may be found in the online version of this article.

Correspondence to:

Y. Terleth,
yterleth@uidaho.edu

Citation:

Terleth, Y., Bartholomaus, T. C., Enderlin, E., Mikesell, T. D., & Liu, J. (2024). Glacier surges and seasonal speedups integrated into a single, enthalpy-based model framework. *Geophysical Research Letters*, *51*, e2024GL112514. https://doi.org/10.1029/2024GL112514

Received 12 SEP 2024
Accepted 26 NOV 2024

Author Contributions:

Conceptualization: Y. Terleth, T. C. Bartholomaus, J. Liu
Data curation: Y. Terleth, T. C. Bartholomaus
Formal analysis: Y. Terleth
Funding acquisition: T. C. Bartholomaus, E. Enderlin, T. D. Mikesell
Investigation: Y. Terleth
Methodology: Y. Terleth, T. C. Bartholomaus
Project administration: T. C. Bartholomaus, E. Enderlin
Resources: T. C. Bartholomaus, E. Enderlin, T. D. Mikesell
Software: Y. Terleth
Supervision: T. C. Bartholomaus, E. Enderlin, T. D. Mikesell

1. Introduction

Glacier velocities vary from sub-daily (Guerin et al., 2021; Stevens et al., 2022) to centennial timescales (Engelhardt & Kamb, 2013; Van Pelt et al., 2012), with magnitudes ranging from centimeters per day (Iken & Bindschadler, 1986) to tens of meters per day (Kamb et al., 1985). Surge-type glaciers are traditionally classified categorically as those glaciers undergoing oscillations in flow speed with multi-year periods, and make up ~1% of world glaciers by number (e.g., Meier & Post, 1969; Truffer et al., 2021). However, recent observations reveal many instances where sub-seasonal and annual velocity variations are superimposed onto the surge-cycle (e.g., Beaud et al., 2022; Benn et al., 2023; Liu et al., 2024), as well as examples of multi-year velocity oscillations that overlay seasonal patterns, but do not fully qualify as surges under the criteria laid out in Meier and Post (1969) (e.g., Herreid & Truffer, 2016). Such a diversity in speedup return periods and amplitudes confounds straightforward, binary surge-type and non-surge-type classifications. In the context of such a spectrum of unsteady flow patterns on multi-year to decadal timescales, what has traditionally been referred to as a "surge" might simply represent the most noticeable manifestation of multi-year oscillatory ice flow (Herreid & Truffer, 2016; Terleth et al., 2024).

The enthalpy model assembles multiple individually suggested mechanisms that contribute to oscillatory ice flow within a single framework (Benn et al., 2019; Sevestre & Benn, 2015). Enthalpy is measured as ice temperature when below the pressure melting point, and as water content when at the pressure melting point

Validation: Y. Terleth
Visualization: Y. Terleth
Writing – original draft: Y. Terleth
Writing – review & editing: Y. Terleth, T. C. Bartholomaus, E. Enderlin, T. D. Mikesell, J. Liu

(Aschwanden et al., 2012). Enthalpy provides a method to quantify and monitor the energy internal to the glacier irrespective of thermal regime. Frictional heating, geothermal heating, and water input contribute positively to the amount of enthalpy at the glacier bed, while heat transfer from the bed to the surface and basal water drainage decrease enthalpy (Benn et al., 2019). Rather than proposing new ice flow mechanics, the enthalpy framework has the merit of providing a single unifying measure of the state of the glacier base, enabling the consideration of oscillatory behavior across a continuous spectrum without a priori categorization (surging vs. non surging, or Svalbard-type vs. Alaska-type) (Benn et al., 2023; Terleth et al., 2021).

Current numerical implementations of the enthalpy model are effective at identifying the envelope of climatic conditions and geometries within which surging occurs (Benn et al., 2019, 2023; Sevestre & Benn, 2015). However, they have not considered significant aspects of the complexity observed during real surge cycles. In this paper, we focus on two distinct but related limitations, both identified in Benn et al. (2023): (a) The current enthalpy model implementation does not include seasonal velocity variability, leading non-surge type glaciers to have uniform, steady speeds and surging glaciers to have a simple velocity spike amidst multiple years of near-steady, "quiescent" flow (i.e., that between surges). Meanwhile, glaciers universally exhibit seasonal changes in flow (e.g., Boxall et al., 2022; Solgaard et al., 2022) and velocity records of surge-type glaciers show seasonal variations in ice flow velocity persist amid the multi-year fluctuations in flow that define surging events (Beaud et al., 2022; Benn et al., 2023; Bindschadler et al., 1977; Liu et al., 2024). (b) In the current enthalpy model, liquid water fluxes to and away from the glacier bed are very low during the quiescent phase. Although surface melt is produced continuously, the penetration of liquid water to the bed depends on ice velocity through a crevassing function, and some model simulations have <1% of surface melt reaching the glacier bed (Benn et al., 2019). As a result, no basal water drainage develops until a tipping point is reached and the bed is fully drained at surge termination. This model behavior does not capture important elements of glacier kinematics nor the observations that subglacial discharge varies with surface runoff even during quiescence (Bouchayer et al., 2023; Kamb & Engelhardt, 1987; Liu et al., 2024; Terleth et al., 2024).

Here, we build upon the numerical implementation of the enthalpy model outlined in Benn et al. (2019) by (a) introducing seasonality in the air temperature forcing, (b) implementing different minimum values of surface-to-distributed drainage system water transfer, and (c) varying the subglacial hydraulic transmissivity. These modifications show that, in addition to an envelope of climatic conditions favorable to surging, glacier-specific attributes determine whether surging occurs. The model reproduces realistic surge-like behavior in ice flow velocity that, importantly, includes seasonal variation in ice flow and in water exchange with the surrounding environment. We discuss the resemblance of the modeled behavior to reality as well as possible implications for our understanding of cyclic ice flow instabilities.

2. Numerical Model

The model of Benn et al. (2019, 2023) is time-dependent but spatially invariant. Here, we begin by briefly summarizing the existing model, then describe specifics to this study within subsequent subsections. The rate of change of ice thickness H is

$$\frac{dH}{dt} = a - m - \frac{Q_i}{l}, \tag{1}$$

where a and m are the net annual accumulation and ablation rates. Q_i is the ice flux, and l is the glacier length. The rate of change of basal enthalpy E is

$$\frac{dE}{dt} = \tau u + G + \rho_i L_f \beta m - Q_{cond} - \frac{\rho_i L_f Q_w}{l}, \tag{2}$$

where τ is the basal shear stress, u is the rate of basal motion, and G is the geothermal heat flux. The ice density ρ_i and latent heat of fusion L_f account for enthalpy supplied to the bed by surface melt, scaled by a factor β, which represents the fraction of water reaching the glacier bed as a linear function of basal motion rate (Section 2.1). Q_{cond} is conductive cooling and Q_w is the water flux draining away from the bed (Section 2.2). The rate of basal

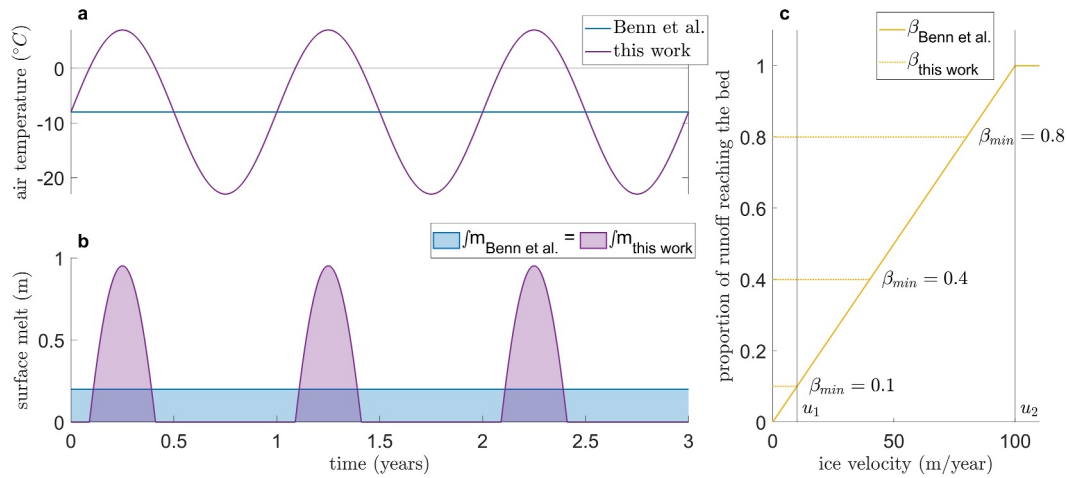

Figure 1. Summary of introduction of seasonality into the model. (a, b) Temperature and surface melt vary on a seasonal cycle. The annual volume of melt produced remains unchanged compared to Benn et al. (2019). (c) β is the fraction of surface melt transferred through the glacier to the distributed drainage system depending on basal motion. Dotted lines show the functions using different values of $\beta_{\min}$, the minimum fraction of surface melt transferred to the bed regardless of ice velocity.

motion, u, is derived from a generalized Weertman-type sliding law under the assumption that the basal shear stress is equal to the driving stress and the effective pressure is simplified to an inverse relationship with the thickness of the basal water layer.

Beyond this general introduction, we refer the reader to Benn et al. (2019) for a detailed model description and numerical implementation, as well as Table S1 in Supporting Information S1 for an overview of the parameters used here. The following subsections describe the two main changes to the model forcing: varying water supply to the glacier bed and increasing the range in basal drainage.

2.1. Water Supply to the Glacier Bed

We calculate melt from air temperature with a positive degree day factor, defined to ensure that the yearly melt volume remains equal to the yearly melt volume in Benn et al. (2019) under equal climatic conditions (Figure 1). To add seasonality in the air temperature and the corresponding surface melt signals, we make the air temperature T a periodic function of time t, measured in years:

$$T(t) = T_a + \mu \sin(2\pi t), \tag{3}$$

where T_a is the annual average temperature, and μ is the amplitude of annual temperature oscillations. The fraction of surface melt reaching the glacier bed is controlled by the ramp-function β, which describes an ice velocity-dependent crevassing extent (Benn et al., 2019). The variable β describes that portion of supraglacial water that accesses the bed, interacts with the subglacial hydrologic system, and can impact ice dynamics. Therefore, $1 - \beta$ is that portion routed around, over, or through the glacier without interacting with the modeled subglacial hydrologic system. We note that this $1 - \beta$ share of the surface melt could include water routed into large moulins that feed directly into well-developed, efficient subglacial channels and that passes through the glacier with very little effect on ice dynamics (e.g., Andrews et al., 2014; Bartholomaus et al., 2011; de Fleurian & Langebroek, 2023; Flowers & Clarke, 2002a). As in Benn et al. (2019), when ice velocity increases, the glacier surface becomes more irregular and crevassed, disrupting supraglacial water flow to discrete moulins and promoting spatially distributed englacial water transfer. We suggest that this transition from point-source to distributed water delivery to the glacier bed is what matters most in the crevassing feedback, rather than the total volume of surface melt transferred to the bed (e.g., Dunse et al., 2015; Sevestre et al., 2018). Furthermore, we make an addition to the definition of β relative to Benn et al. (2019). We set:

$$\beta = \begin{cases} \min\left(\beta_{\min}, \dfrac{u - u_1}{u_2 - u_1}\right) & \text{if } u < u_2, \\ 1 & \text{if } u \geq u_2. \end{cases} \quad (4)$$

The value of u_1 describes the rate of basal motion at which crevassing expands beyond a baseline extent, and u_2 describes that velocity at which crevassing entirely disrupts the formation of distinct supraglacial streams that interact with crevasses to form moulins.

Decreasing u_1 and u_2 allows a larger share of surface melt to directly enter the modeled hydrological system, but doing so reduces the potential for water transfer to the glacier bed to increase with surge onset as described in for example, Dunse et al. (2015). Additionally, u_1 and u_2 are poorly-constrained parameters with little observational basis. In this work, we leave u_1 and u_2 fixed at 10 m/year and 100 m/year, respectively, and define $\beta_{\min}$ as the minimum fraction of surface melt that reaches the subglacial distributed hydrologic system, ranging from 0 to 1, even at low rates of basal motion. As such, the distinction we make compared to Benn et al. (2019) is that we allow for non-zero water inputs when there is normal baseline crevassing through $\beta_{\min}$.

2.2. Basal Drainage

Basal drainage is described following Benn et al. (2019):

$$Q_w = K(\rho_i g \sin\theta) w^{\alpha} + \phi \frac{K_c}{W_c}(\rho_i g \sin\theta)^{1/2} S^{4/3}. \quad (5)$$

The first term on the right hand side describes the distributed drainage component, which is driven by a gravitational gradient ($\rho_i g \sin\theta$, with θ the glacier bed slope, equal to the surface slope) and strongly dependent ($\alpha = 5$) on the thickness of the water film w (Flowers & Clarke, 2002b). K is a free parameter describing the basal hydraulic transmissivity, encapsulating several different basal characteristics that affect how easily liquid water diffuses through the subglacial environment (Benn et al., 2019). This includes the hydraulic conductivity of subglacial tills (Fischer et al., 2001; Hubbard & Maltman, 2000) and the effects of small scale bed roughness on subglacial water flow (e.g., Creyts & Schoof, 2009). The properties of the subglacial bed may vary among glaciers, so we explore the effect of varying K, as done in Benn et al. (2019). We refer to K as a multiple of its value in Benn et al. (2019), K_0 ($K_0 = 2.3 \times 10^{-47}$ kg^{-5} m^2 s^9). We consider values of K that range between $0.005 \times K_0$ and $10 \times K_0$, nearly four orders of magnitude, similar to the range of reported subglacial hydraulic transmissivities (e.g., Iken et al., 1996; Kulessa & Murray, 2003; Lai et al., 2021; Sommers et al., 2023).

The second term on the right hand side describes the channelized drainage component, also driven by a gravitational gradient. ϕ is a fill-fraction allowing the channels to be partially filled during times of falling discharge (Benn et al., 2019). K_c is a constant describing channel roughness, W_c is a constant describing channel spacing, and S describes channel cross sectional area.

3. Results

3.1. Seasonally Variable Water Supply to the Glacier Base

We reproduce the previously published surging behavior using the model setup of Benn et al. (2019), with annual accumulation of 0.6 m.w.e. and mean annual temperature of −8°C (Figure S1 in Supporting Information S1). However, when we introduce seasonality in meltwater production and the modified meltwater supply to the bed, surges no longer occur without further modification to the model. The model output shifts from sudden speedups every ∼8 years (Figure 2a) to a regime of annual speedups driven by the melt season influx of surface runoff (Figure 2b). Each year, surface melt reaches the bed when temperatures rise above freezing, but ice speeds are low and only 10% of surface runoff is transferred to the glacier bed (Figure 2b). The seasonal initiation of melt input increases basal enthalpy, lowers effective pressure, and accelerates ice-velocities, triggering an acceleration akin to a "spring speed up" (e.g., Anderson et al., 2004; Mair et al., 2003). Increased basal water thickness (w) briefly drives significant drainage from the distributed component of the drainage network (Equation 5), followed by a drop in ice-velocities. Thus, seasonal enthalpy gains also dissipate seasonally.

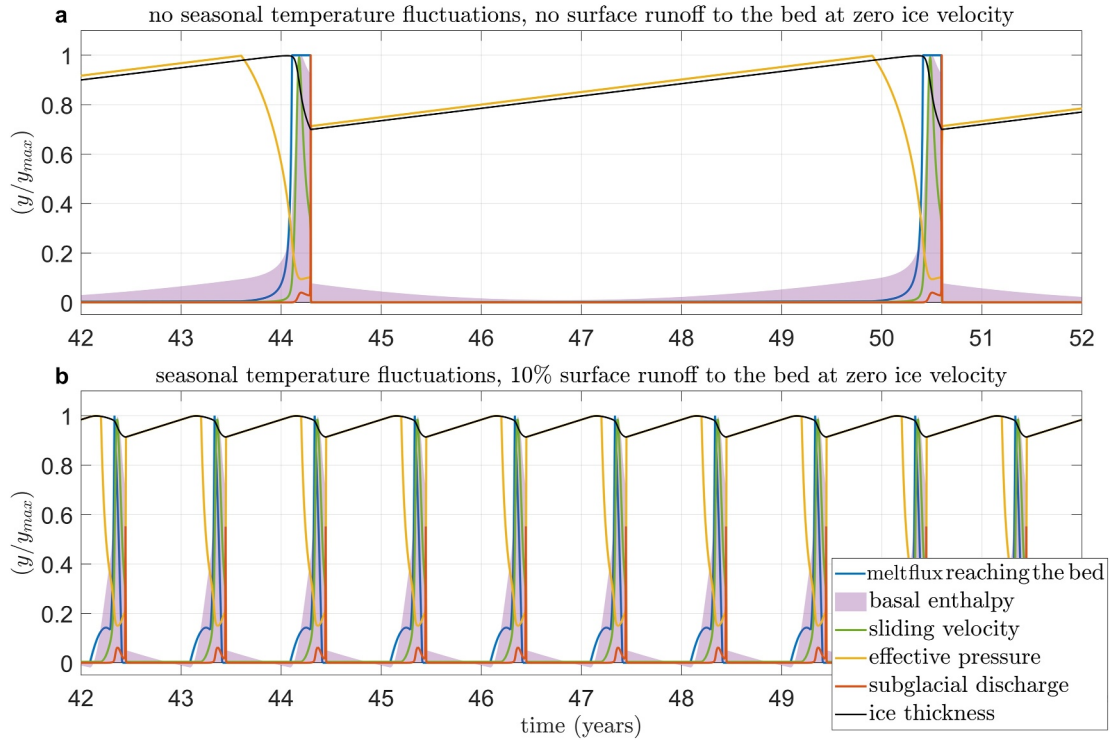

Figure 2. Comparison of output variable timeseries for two model realizations, both with the same climatic parameters. All variables are normalized by their respective maximum values. (a) Case with $\beta_{min} = 0$ and no seasonal temperature fluctuations. This corresponds to Case 3 in Benn et al. (2019). (b) Case with the introduction of seasonal temperature fluctuations and where at least 10% of surface meltwater reaches the glacier bed at all times.

3.2. Variation in Distributed Drainage System Supply and Hydraulic Transmissivity

Our model solutions exhibit a wide range of behaviors dependent on choices for β_{min} and K (Figure 3). All model solutions for $\beta_{min} > 0$ contain annual oscillations in ice velocity, thickness, and other characteristics. To describe longer-timescale oscillations, we identify the return period of maxima in sliding velocity (or equivalently, ice thickness). All parameter combinations to the left of the 2-year contour in Figure 3a ($\sim$15% of the investigated parameter space) contain oscillatory behavior with a return period of 2 years or more. The longest return period in the parameter space is >1,500 years, for $\beta_{min} = 0$ and $K = 0.005 \times K_0$. Return periods decrease rapidly with increasing values of K. Return periods also decrease with increasing values of β_{min}. At $K = 0.005 \times K_0$, $\beta_{min} = 0.075$ yields 100-year surge intervals, and $\beta_{min} = 0.12$ yields 10-year surge intervals. As β_{min} increases, increasingly low values of K are needed to produce multi-year speedups, and vice-versa. However, the dependence of return period on K and β_{min} is not consistent everywhere, and sets of these parameters produce only seasonally varying velocities (e.g., $K < 0.2 \times K_0$ with $\beta_{min} > 0.12$, Figure S3 in Supporting Information S1). We quantify the duration of the active phase of the surge cycle by the duration of dynamic thinning (Text S2, Figure S2 in Supporting Information S1). The duration of dynamic thinning varies between <1 year and $\sim$22 years, depending on K and β_{min}, but with a different functional relationship than that of surge recurrence. Surge recurrence and surge duration are independent. Lower values of K tend to drive longer surges (Figure S4 in Supporting Information S1), while the dependence on water delivery to the distributed system during quiescent phases (β_{min}) is more complicated.

3.3. Modeled Surge Cycle

Here we discuss one specific parameter combination of $\beta_{min} = 0.1$ and $K = 0.01 \times K_0$ to demonstrate new insights provided by the modified enthalpy model. This parameter combination produces surges every 16 years with 3.3 years durations, and its solutions are representative of a wider range of the parameter space (Figure 3). More unusual results that are uncommon within the $K - \beta_{min}$ phase space, including non-periodic behavior, are

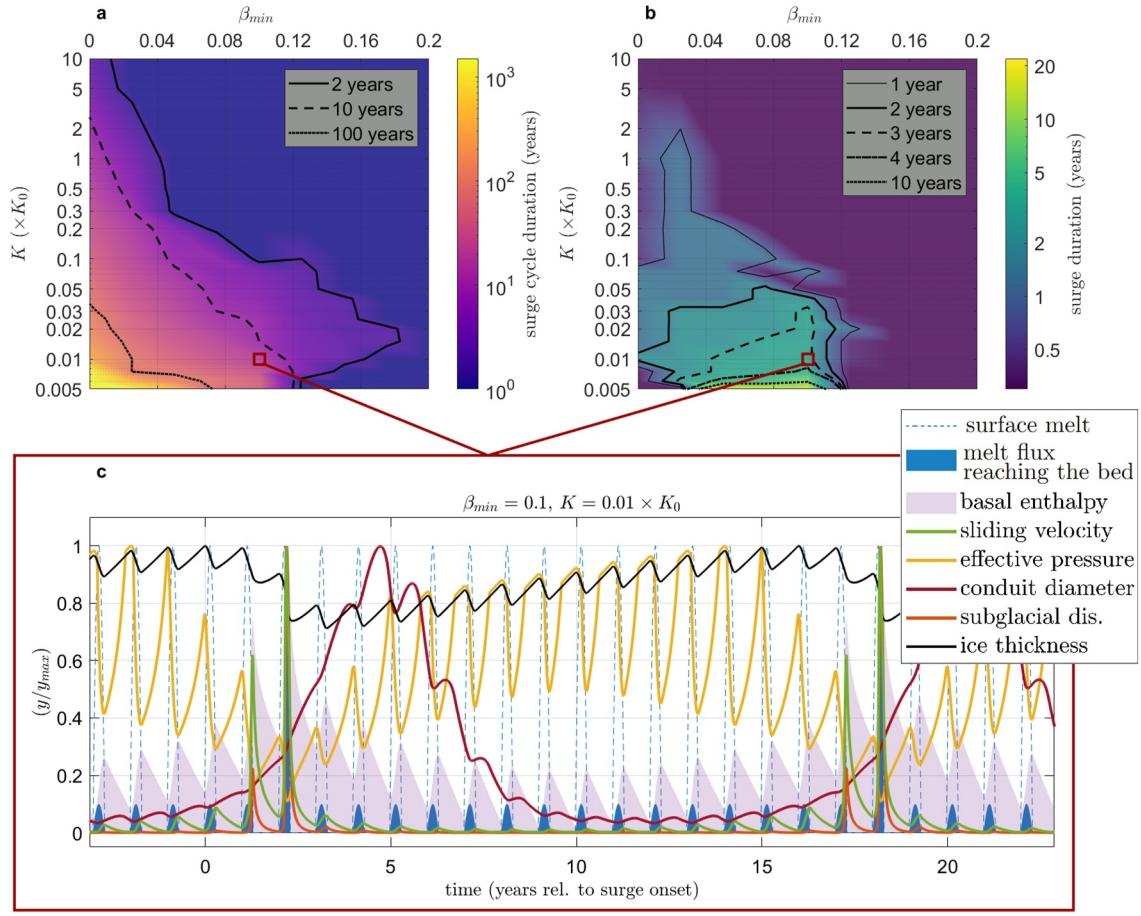

Figure 3. (a) Return period of the highest amplitude speedup present in the modeled basal motion as a function of $\beta_{\min}$ and K. Solid contour shows a 2-year return interval (i.e., the shortest potential return period that could be identified as a surge) and dotted contours indicate 10-year and 100-year return intervals. No dynamically stable model solutions exist below $K = 0.005 \times K_0$ (Figure S2 in Supporting Information S1). Only seasonal speedups are produced when $\beta_{\min} > 0.25$. (b) Surge duration, determined as the time interval between the maximum modeled ice thickness and the consecutive minimum modeled ice thickness, as a function of $\beta_{\min}$ and K. Note the Y-axis and color-map are on logarithmic scales. (c) Model solution for $\beta_{\min} = 0.1$ and $K = 0.01 \times K_0$. All variables normalized by their respective maximum values, and time is defined relative to the first year with a clear peak in sliding velocity. Legend as in Figure 2.

presented within the Supporting Information S1. The first half of quiescent phases (e.g., year 3–year 10 in Figure 3c) show net, but non-monotonic decreases in basal enthalpy. The second half of quiescent phases (e.g., year 11–year 16) are marked by net, but non-monotonic, accumulation of basal enthalpy. Seasonally evolving channel size is present throughout the quiescent phase. The melt season influx of water to the distributed drainage system causes decreasing annual minima in effective pressure from 50% of its maximum value in year 11 in Figure 3c (5 years prior to surging) to 25% of its maximum value in year 16 (at surge initiation). During this time, seasonality in conduit diameter is superimposed on a multi-year pattern that sees channel size peak ~1.5 years after surge termination (year 4.5 in Figure 3c), then decrease to ~5% of the maximum value by year 9. Over the 5 years leading up to the next surge, the conduit diameter increases to ~15% of its maximum value. In years 0 and 16 (the years of surge initiation), the wintertime effective pressure remains below 80% of the ice overburden pressure, allowing increased wintertime basal motion. The surge then materializes as a 3.28 year period of dynamic thinning and ~10-fold increases in ice velocity, with above quiescent wintertime velocities maintained between the two surge summers (Figure 3c). The subglacial discharge volume increases during the surge summers, reaching up to 100-fold its summertime quiescent levels. Mid-surge peak subglacial discharge is largely accommodated by the distributed drainage system, although the channel size continues to grow during and several years after the surge. At the conclusion of the three surge years, basal enthalpy remains above ~40% of its maximal value and wintertime effective pressure remains below 40% of overburden pressure. However, ice

thickness has decreased by ∼30%, leading to lower driving stress, and the subsequent melt-season speedup has a lower magnitude. Because basal enthalpy (i.e., subglacial water content) remains high, there is continued growth of the channelized drainage component until year 4 (∼1.5 years after the surge). Wintertime basal enthalpy decreases to reach values near zero nearly halfway through quiescence. Wintertime effective pressure increases after the surge to match overburden pressure by year 5 (∼2 years after the surge) (Figure 3c).

4. Discussion

While the model results show that certain parameter combinations of low basal hydraulic transmissivity and restricted water supply to the distributed drainage system yield both annual and multi-year variability in ice velocities (Figure 3), we acknowledge the simplified physics when trying to infer quantitative meaning from these values. For example, the basal transmissivity parameter K encompasses multiple processes: we do not untangle the respective roles of subglacial roughness and till porosity, and there are likely non-linear behaviors and responses within each of these characteristics that we do not account for here (e.g., Beaud et al., 2022; Minchew & Meyer, 2020; Thøgersen et al., 2019). Climate is also known to impact the occurrence of surges (Sevestre & Benn, 2015), which in this framework would impact the pacing of water delivery to the bed in ways potentially similar to our K and $\beta_{\min}$ parameters. We do not explore the relationships between climate and surge characteristics here. Additionally, the simplistic nature of the model prevents any evaluation of spatial heterogeneity in drainage, crevassing extent, or friction characteristics even though these characteristics could be crucial to the surging mechanism(s) (e.g., Haga et al., 2020).

Despite the simplified physics of the model, the simulated oscillations in glacier velocity, thickness, and drainage resemble realistic surge cycles. We simulate seasonal speedups that escalate in amplitude in the lead up to the surge (Figure 3b), consistent with observations (Liu et al., 2024; Raymond & Harrison, 1988). The increasing amplitude of the modeled seasonal speedups are driven by gradually accumulating basal enthalpy, which results from an excess of basal water supply relative to basal drainage and a gradual increase in ice thickness and driving stress (Text S4 in Supporting Information S1). The crevassing feedback (Dunse et al., 2015; Sevestre et al., 2018) in the model accentuates surging by driving a rapid increase in surface water delivery to the distributed drainage system (year one in Figure 3b). We model active phases that last between <1 and ∼22 years (Figure 3b) and that show continued seasonal fluctuations in the drainage system discharge and in glacier velocities (Figure 3c), also reflecting observations (Benn et al., 2023; Liu et al., 2024; Terleth et al., 2024). At the end of modeled surges, effective pressure remains low, the volume of basal water remains above 50% of the surge-time maximum, and the channelized drainage system continues to grow (Figure 3c). Because the model permits surge termination prior to the full drainage of the glacier bed, the simulations show continuous and seasonally varying subglacial discharge, plus gradual drainage of the glacier bed in the years following the surge, further mirroring field observations (Terleth et al., 2024; Zhan, 2019). Surge termination in the model is driven by a combination of improved drainage and a ∼30% reduction in driving stress that results from dynamic thinning of the glacier during the surge (Figure S5 in Supporting Information S1). The influence of driving stress in surge termination agrees with numerous observations of mass depletion from the reservoir zone (e.g., Guillet et al., 2022; Jiskoot et al., 2001; Lauzon et al., 2023; Nolan et al., 2021). While surge initiation has long been explicitly linked to critical driving stress values in the reservoir zone (Eisen et al., 2005; Liu et al., 2024), our novel model results strengthen the notion that the interplay of subglacial hydrology and changes in driving stress drive the entire surge cycle, including surge termination.

The notion that basal water trapped in a distributed subglacial drainage system drives surging is long-standing (Fowler, 1987; Kamb, 1987; Kamb et al., 1985). However, the mechanism exhibited by the enthalpy model is different from earlier theories of hydrologically-driven surging in that the poorly-drained distributed drainage system plays a key role in priming the glacier to surge, rather than during the surge itself. Our model implementation retains the Benn et al. (2019) characteristic that surges are the result of a mass and enthalpy build-up during the quiescent phase, and shows that this process can persist under seasonally evolving basal drainage. Parameter combinations that limit water supply to the distributed drainage system during quiescence $(\beta_{\min})$ and limit the connectivity of the distributed drainage system (K) are required to produce surges in the model. The surge phase is then marked by a period of active subglacial water drainage prior to surge termination, reflecting field observations (Terleth et al., 2024). In the model, the water supply $(\beta_{\min} < 0.12)$ from

surface melt and basal hydraulic transmissivity (K) must be restricted such that there is insufficient water flux during quiescence to "flush and drain" the distributed system annually, allowing basal enthalpy to accumulate (Equation 5). The root of the unusual behavior of surge-type glaciers may thus lie in their quiescent dynamics, rather than in their surging dynamics, when water drainage is more similar to the mid-summer configuration of a non-surging glacier.

Fine-grained, soft, basal sediments are one source of low hydraulic transmissivity conditions (e.g., Doyle et al., 2022; Flowers & Clarke, 2002a; Stone & Clarke, 1993) and are found at the bed of most surging glaciers (Harrison & Post, 2003). Surging occurrence has been explicitly linked to soft beds (Bouchayer et al., 2023; Jiskoot et al., 1998; Murray et al., 2000), although such trends might also reflect the low shear strength of tills aiding fast basal motion (Truffer et al., 2000) rather than only hydrological characteristics. Meanwhile, our results demonstrate that no distinguishable features of the basal drainage system need be present that separate surge-type glaciers from non-surge-type glaciers (Raymond et al., 1995). To draw more definitive conclusions, future work could consider spatial heterogeneity in the drainage system during quiescence. For example, Crompton et al. (2018) suggest that transitions from harder substrates to soft beds below the glacier might provide advantageous conditions for surging. Furthermore, basal hydraulic transmissivity has been suggested to be strongly variable over glacier beds (e.g., Rada Giacaman & Schoof, 2023; Sommers et al., 2023), and spatially distributed modeling could prove helpful in determining the configuration and required extent of low-transmissivity conditions that promote surging (e.g., Tsai et al., 2022).

In addition to the envelope of climatic conditions favorable to surging suggested in Benn et al. (2019), our model results suggest that glacier specific water supply and drainage characteristics (e.g., $\beta_{\min}$ and K) influence the propensity to surging and the duration of the surge cycle. While the impact of K on surge propensity was identified previously Benn et al. (2019), lower values of both parameters produce longer surge recurrence intervals (Figure 3a) but the active phase duration decreases with K (Figure 3b, Text S5 in Supporting Information S1). These glacier-specific factors might help explain why surging and non-surging glaciers exist in close proximity under similar climates (e.g., Guillet et al., 2022; Post, 1969; Sevestre & Benn, 2015). The model solutions in Figure 3c newly capture several key features that have been observed for surging glaciers. First, annual, seasonally-driven oscillations in ice velocities persist throughout the quiescent and surging phases of the surge cycle. Second, water flux continues through the basal environment during all stages of the surge cycle. Importantly, there is a continuum of seasonal to multi-year speedups that arise naturally from the model, and that are achieved with the same effective pressure-dependent, monotonic sliding law. While we certainly do not discard the possible importance of ice velocity-weakening basal resistance to flow as a mechanism for surging (Minchew & Meyer, 2020; Thøgersen et al., 2019, 2024), it is noteworthy that such behavior is not needed to produce surges in our model. There is also no need for a dramatic change in the characteristics of the subglacial hydrologic network, such as a sudden transition from channelized to distributed drainage (Kamb, 1987), to trigger or terminate surging. Instead, our model suggests that surges can be the expression of a combination of circumstances occurring throughout the surge cycle and described by a single physical system, rather than requiring more complicated surge-specific binary ice flow mechanics.

5. Conclusion

Our model results show that a simple, periodic, hydrological forcing can drive variability in ice velocity at multiple timescales simultaneously. Using the basal enthalpy-driven surge cycle of Benn et al. (2019) as a starting point and working from fixed climatic parameters with seasonally variable surface melt, we investigated the effect of varying the minimum fraction of surface melt reaching the distributed basal drainage system and the hydraulic transmissivity of the distributed drainage system. We produce seasonal oscillations in ice velocity throughout the investigated parameter space. Additionally, smaller portions (<12%) of surface melt consistently supplied directly to the distributed drainage system, combined with subglacial environments that have low hydraulic transmissivities favor surging in our model. Conversely, lower portions of supraglacial water that interact with the subglacial drainage system and more transmissive distributed systems inhibit surges. Our findings are derived from simulations made with a simplified zero-dimensional model. Nevertheless, the features we identify show many similarities to both observed surges and non-surge-type glaciers, and our extended model provides a physically-based, straight-forward explanation for diverse, temporal patterns in glacier velocity.

Data Availability Statement

A Matlab version of the enthalpy model and the model solutions presented here are archived at Terleth and Bartholomaus (2024).

Acknowledgments
This work was funded through the NSF Arctic Natural Sciences program, via awards 1954021 and 1954006. TDM acknowledges basic funding support to NGI from The Research Council of Norway. We would like to thank Martin Truffer and Elizabeth Cassel for helpful discussions leading to this manuscript. We would also like to thank one anonymous reviewer and Doug Benn for an insightful and constructive review. Finally, our work on this wider project received immense support from the late Hans Munich and Tanya Hutchins at Coastal Airline Services LLC.

References

Anderson, R. S., Anderson, S. P., MacGregor, K. R., Waddington, E. D., O'Neel, S., Riihimaki, C. A., & Loso, M. G. (2004). Strong feedbacks between hydrology and sliding of a small alpine glacier. *Journal of Geophysical Research*, *109*(F3). https://doi.org/10.1029/2004JF000120

Andrews, L. C., Catania, G. A., Hoffman, M. J., Gulley, J. D., Lüthi, M. P., Ryser, C., et al. (2014). Direct observations of evolving subglacial drainage beneath the Greenland Ice Sheet. *Nature*, *514*(7520), 80–83. https://doi.org/10.1038/nature13796

Aschwanden, A., Bueler, E., Khroulev, C., & Blatter, H. (2012). An enthalpy formulation for glaciers and ice sheets. *Journal of Glaciology*, *58*(209), 441–457. https://doi.org/10.3189/2012JoG11J088

Bartholomaus, T. C., Anderson, R. S., & Anderson, S. P. (2011). Growth and collapse of the distributed subglacial hydrologic system of Kennicott Glacier, Alaska, USA, and its effects on basal motion. *Journal of Glaciology*, *57*(206), 985–1002. https://doi.org/10.3189/002214311798843269

Beaud, F., Aati, S., Delaney, I., Adhikari, S., & Avouac, J.-P. (2022). Surge dynamics of Shisper Glacier revealed by time-series correlation of optical satellite images and their utility to substantiate a generalized sliding law. *The Cryosphere*, *16*(8), 3123–3148. https://doi.org/10.5194/tc-16-3123-2022

Benn, D., Fowler, A. C., Hewitt, I., & Sevestre, H. (2019). A general theory of glacier surges. *Journal of Glaciology*, *65*(253), 701–716. https://doi.org/10.1017/jog.2019.62

Benn, D., Hewitt, I. J., & Luckman, A. J. (2023). Enthalpy balance theory unifies diverse glacier surge behaviour. *Annals of Glaciology*, *63*(87–89), 1–7. https://doi.org/10.1017/aog.2023.23

Bindschadler, R., Harrison, W. D., Raymond, C. F., & Crosson, R. (1977). Geometry and dynamics of a surge-type glacier. *Journal of Glaciology*, *18*(79), 181–194. https://doi.org/10.3189/S0022143000021298

Bouchayer, C., Nanni, U., Lefeuvre, P.-M., Hulth, J., Steffensen Schmidt, L., Kohler, J., et al. (2023). Multi-scale variations of hydro-mechanical conditions at the base of the surge-type glacier Kongsvegen. *Svalbard. EGUsphere*, 1–41. https://doi.org/10.5194/egusphere-2023-618

Boxall, K., Christie, F. D., Willis, I. C., Wuite, J., & Nagler, T. (2022). Seasonal land-ice-flow variability in the Antarctic Peninsula. *The Cryosphere*, *16*(10), 3907–3932. https://doi.org/10.5194/tc-16-3907-2022

Creyts, T. T., & Schoof, C. G. (2009). Drainage through subglacial water sheets. *Journal of Geophysical Research*, *114*(F4). https://doi.org/10.1029/2008JF001215

Crompton, J. W., Flowers, G. E., & Stead, D. (2018). Bedrock fracture characteristics as a possible control on the distribution of surge-type glaciers. *Journal of Geophysical Research: Earth Surface*, *123*(5), 853–873. https://doi.org/10.1002/2017JF004505

de Fleurian, B., & Langebroek, P. (2023). Moulin density impacts the effect of subglacial hydrology on ice dynamics. *ESS Open Archive (preprint)*. https://doi.org/10.22541/essoar.167979642.20528063/v1

Doyle, S. H., Hubbard, B., Christoffersen, P., Law, R., Hewitt, D. R., Neufeld, J. A., et al. (2022). Water flow through sediments and at the ice-sediment interface beneath sermeq Kujalleq (Store glacier), Greenland. *Journal of Glaciology*, *68*(270), 665–684. https://doi.org/10.1017/jog.2021.121

Dunse, T., Schellenberger, T., Hagen, J. O. M., Kääb, A., Schuler, T. V., & Reijmer, C. (2015). Glacier-surge mechanisms promoted by a hydro-thermodynamic feedback to summer melt. *The Cryosphere*, *9*(1), 197–215. https://doi.org/10.5194/tc-9-197-2015

Eisen, O., Harrison, W. D., Raymond, C. F., Echelmeyer, K. A., Bender, G. A., & Gorda, J. L. (2005). Variegated Glacier, Alaska, USA: A century of surges. *Journal of Glaciology*, *51*(174), 399–406. https://doi.org/10.3189/172756505781829250

Engelhardt, H., & Kamb, B. (2013). Kamb Ice Stream flow history and surge potential. *Annals of Glaciology*, *54*(63), 287–298. https://doi.org/10.3189/2013AoG63A535

Fischer, U. H., Porter, P. R., Schuler, T., Evans, A. J., & Gudmundsson, G. H. (2001). Hydraulic and mechanical properties of glacial sediments beneath Unteraargletscher, Switzerland: Implications for glacier basal motion. *Hydrological Processes*, *15*(18), 3525–3540. https://doi.org/10.1002/hyp.349

Flowers, G. E., & Clarke, G. K. C. (2002a). A multicomponent coupled model of glacier hydrology 1. Theory and synthetic examples. *Journal of Geophysical Research*, *107*(B11), ECV9-1–ECV9-17. https://doi.org/10.1029/2001JB001122

Flowers, G. E., & Clarke, G. K. C. (2002b). A multicomponent coupled model of glacier hydrology 2. Application to Trapridge Glacier, Yukon, Canada. *Journal of Geophysical Research*, *107*(B11), ECV10-1–ECV10-16. https://doi.org/10.1029/2001JB001124

Fowler, A. C. (1987). A theory of glacier surges. *Journal of Geophysical Research*, *92*(B9), 9111–9120. https://doi.org/10.1029/JB092iB09p09111

Guerin, G., Mordret, A., Rivet, D., Lipovsky, B. P., & Minchew, B. M. (2021). Frictional origin of slip events of the Whillans ice stream, Antarctica. *Geophysical Research Letters*, *48*(11), e2021GL092950. https://doi.org/10.1029/2021GL092950

Guillet, G., King, O., Lv, M., Ghuffar, S., Benn, D., Quincey, D., & Bolch, T. (2022). A regionally resolved inventory of High Mountain Asia surge-type glaciers, derived from a multi-factor remote sensing approach. *The Cryosphere*, *16*(2), 603–623. https://doi.org/10.5194/tc-16-603-2022

Haga, O. N., McNabb, R., Nuth, C., Altena, B., Schellenberger, T., & Kääb, A. (2020). From high friction zone to frontal collapse: Dynamics of an ongoing tidewater glacier surge. *Negribreen, Svalbard. Journal of Glaciology*, 1–13. https://doi.org/10.1017/jog.2020.43

Harrison, W. D., & Post, A. S. (2003). How much do we really know about glacier surging? *Annals of Glaciology*, *36*, 1–6. https://doi.org/10.3189/172756403781816185

Herreid, S., & Truffer, M. (2016). Automated detection of unstable glacier flow and a spectrum of speedup behavior in the Alaska Range. *Journal of Geophysical Research: Earth Surface*, *121*(1), 64–81. https://doi.org/10.1002/2015JF003502

Hubbard, B., & Maltman, A. (2000). Laboratory investigations of the strength, static hydraulic conductivity and dynamic hydraulic conductivity of glacial sediments. *Geological Society, London, Special Publications*, *176*(1), 231–242. https://doi.org/10.1144/GSL.SP.2000.176.01.18

Iken, A., & Bindschadler, R. A. (1986). Combined measurements of subglacial water pressure and surface velocity of Findelengletscher, Switzerland: Conclusions about drainage system and sliding mechanism. *Journal of Glaciology*, *32*(110), 101–119. https://doi.org/10.3189/S0022143000006936

Iken, A., Fabri, K., & Funk, M. (1996). Water storage and subglacial drainage conditions inferred from borehole measurements on gornergletscher, Valais, Switzerland. *Journal of Glaciology*, *42*(141), 233–248. https://doi.org/10.3189/S0022143000004093

Jiskoot, H., Boyle, P., & Murray, T. (1998). The incidence of glacier surging in Svalbard: Evidence from multivariate statistics. *Computers and Geosciences*, *24*(4), 387–399. https://doi.org/10.1016/S0098-3004(98)00033-8

Jiskoot, H., Pedersen, A. K., & Murray, T. (2001). Multi-model photogrammetric analysis of the 1990s surge of sortebræ, east Greenland. *Journal of Glaciology*, *47*(159), 677–687. https://doi.org/10.3189/172756501781831846

Kamb, B. (1987). Glacier surge mechanism based on linked cavity configuration of the basal water conduit system. *Journal of Geophysical Research*, *92*(B9), 9083–9100. https://doi.org/10.1029/JB092iB09p09083

Kamb, B., & Engelhardt, H. (1987). Waves of Accelerated Motion in a Glacier Approaching Surge: The Mini-Surges of Variegated Glacier, Alaska, U.S.A.*. *Journal of Glaciology*, *33*(113), 27–46. https://doi.org/10.3189/S0022143000005311

Kamb, B., Raymond, C. F., Harrison, W. D., Engelhardt, H., Echelmeyer, K. A., Humphrey, N., et al. (1985). Glacier surge mechanism: 1982-1983 surge of Variegated Glacier, Alaska. *Science*, *227*(4686), 469–479. https://doi.org/10.1126/science.227.4686.469

Kulessa, B., & Murray, T. (2003). Slug-test derived differences in bed hydraulic properties between a surge-type and a non-surge-type Svalbard glacier. *Annals of Glaciology*, *36*, 103–109. https://doi.org/10.3189/172756403781816257

Lai, C.-Y., Stevens, L. A., Chase, D. L., Creyts, T. T., Behn, M. D., Das, S. B., & Stone, H. A. (2021). Hydraulic transmissivity inferred from ice-sheet relaxation following Greenland supraglacial lake drainages. *Nature Communications*, *12*(1), 3955. https://doi.org/10.1038/s41467-021-24186-6

Lauzon, B., Copland, L., Wychen, W. V., Kochtitzky, W., McNabb, R., & Dahl-Jensen, D. (2023). Dynamics throughout a complete surge of Iceberg Glacier on western Axel Heiberg Island, Canadian High Arctic. *Journal of Glaciology*, *69*(277), 1333–1350. https://doi.org/10.1017/jog.2023.20

Liu, J., Enderlin, E. M., Bartholomaus, T. C., Terleth, Y., Mikesell, T. D., & Beaud, F. (2024). Propagating speedups during quiescence escalate to the 2020–2021 surge of Sít' Kusá, southeast Alaska. *Journal of Glaciology*, 1–12. https://doi.org/10.1017/jog.2023.99

Mair, D., Willis, I., Fischer, U. H., Hubbard, B., Nienow, P., & Hubbard, A. (2003). Hydrological controls on patterns of surface, internal and basal motion during three "spring events": Haut glacier D'arolla, Switzerland. *Journal of Glaciology*, *49*(167), 555–567. https://doi.org/10.3189/172756503781830467

Meier, M. F., & Post, A. (1969). What are glacier surges? *Canadian Journal of Earth Sciences*, *6*(4), 807–817. https://doi.org/10.1139/e69-081

Minchew, B. M., & Meyer, C. R. (2020). Dilation of subglacial sediment governs incipient surge motion in glaciers with deformable beds. *Proceedings of the Royal Society A*, *476*(2238), 0033. https://doi.org/10.1098/rspa.2020.0033

Murray, T., Stuart, G. W., Miller, P. J., Woodward, J., Smith, A. M., Porter, P. R., & Jiskoot, H. (2000). Glacier surge propagation by thermal evolution at the bed. *Journal of Geophysical Research*, *105*(B6), 13491–13507. https://doi.org/10.1029/2000JB900066

Nolan, A., Kochtitzky, W., Enderlin, E. M., McNabb, R., & Kreutz, K. J. (2021). Kinematics of the exceptionally-short surge cycles of Sit Kusa (Turner Glacier), Alaska, from 1983 to 2013. *Journal of Glaciology*, *67*(264), 1–15. https://doi.org/10.1017/jog.2021.29

Post, A. (1969). Distribution of surging glaciers in western North America. *Journal of Glaciology*, *8*(53), 229–240. https://doi.org/10.3189/S0022143000031221

Rada Giacaman, C. A., & Schoof, C. (2023). Channelized, distributed, and disconnected: Spatial structure and temporal evolution of the subglacial drainage under a valley glacier in the Yukon. *The Cryosphere*, *17*(2), 761–787. https://doi.org/10.5194/tc-17-761-2023

Raymond, C. F., Benedict, R. J., Harrison, W. D., Echelmeyer, K. A., & Sturm, M. (1995). Hydrological discharges and motion of Fels and Black Rapids Glaciers, Alaska, U.S.A.: Implications for the structure of their drainage systems. *Journal of Glaciology*, *41*(138), 290–304. https://doi.org/10.3189/S002214300001618X

Raymond, C. F., & Harrison, W. (1988). Evolution of variegated glacier, Alaska, USA, prior to its surge. *Journal of Glaciology*, *34*(117), 154–169. https://doi.org/10.3189/S0022143000032184

Sevestre, H., & Benn, D. I. (2015). Climatic and geometric controls on the global distribution of surge-type glaciers: Implications for a unifying model of surging. *Journal of Glaciology*, *61*(228), 646–662. https://doi.org/10.3189/2015JoG14J136

Sevestre, H., Benn, D. I., Luckman, A., Nuth, C., Kohler, J., Lindbäck, K., & Pettersson, R. (2018). Tidewater glacier surges initiated at the terminus. *Journal of Geophysical Research: Earth Surface*, *123*(5), 1035–1051. https://doi.org/10.1029/2017JF004358

Solgaard, A., Rapp, D., Noël, B., & Hvidberg, C. (2022). Seasonal patterns of Greenland ice velocity from sentinel-1 SAR data linked to runoff. *Geophysical Research Letters*, *49*(24), e2022GL100343. https://doi.org/10.1029/2022GL100343

Sommers, A., Meyer, C., Morlighem, M., Rajaram, H., Poinar, K., Chu, W., & Mejia, J. (2023). Subglacial hydrology modeling predicts high winter water pressure and spatially variable transmissivity at Helheim Glacier, Greenland. *Journal of Glaciology*, 1–13. https://doi.org/10.1017/jog.2023.39

Stevens, L. A., Nettles, M., Davis, J. L., Creyts, T. T., Kingslake, J., Ahlstrøm, A. P., & Larsen, T. B. (2022). Helheim Glacier diurnal velocity fluctuations driven by surface melt forcing. *Journal of Glaciology*, *68*(267), 77–89. https://doi.org/10.1017/jog.2021.74

Stone, D. B., & Clarke, G. K. C. (1993). Estimation of subglacial hydraulic properties from induced changes in basal water pressure: A theoretical framework for borehole-response tests. *Journal of Glaciology*, *39*(132), 327–340. https://doi.org/10.3189/S0022143000015999

Terleth, Y., & Bartholomaus, T. C. (2024). Model code and solution dataset for "glacier surges and seasonal speedups integrated into a single, enthalpy-based model framework" [Computational notebook]. *Zenodo*. https://doi.org/10.5281/zenodo.12538180

Terleth, Y., Bartholomaus, T. C., Liu, J., Beaud, F., Mikesell, T. D., & Enderlin, E. M. (2024). Transient subglacial water routing efficiency modulates ice velocities prior to surge termination on Sít' Kusá, Alaska. *Journal of Glaciology*, 1–17. https://doi.org/10.1017/jog.2024.38

Terleth, Y., Van Pelt, W., Pohjola, V., & Pettersson, R. (2021). Complementary approaches towards a universal model of glacier surges. *Frontiers in Earth Science*, *9*. https://doi.org/10.3389/feart.2021.732962

Thøgersen, K., Gilbert, A., Bouchayer, C., & Schuler, T. V. (2024). Glacier surges controlled by the close interplay between subglacial friction and drainage. *Journal of Geophysical Research: Earth Surface*, *129*(10), e2023JF007441. https://doi.org/10.1029/2023JF007441

Thøgersen, K., Gilbert, A., Schuler, T. V., & Malthe-Sørenssen, A. (2019). Rate-and-state friction explains glacier surge propagation. *Nature Communications*, *10*(1), 1–8. https://doi.org/10.1038/s41467-019-10506-4

Truffer, M., Harrison, W. D., & Echelmeyer, K. A. (2000). Glacier motion dominated by processes deep in underlying till. *Journal of Glaciology*, *46*(153), 213–221. https://doi.org/10.3189/172756500781832909

Truffer, M., Kääb, A., Harrison, W. D., Osipova, G. B., Nosenko, G. A., Espizua, L., et al. (2021). Chapter 13 - Glacier surges. In W. Haeberli & C. Whiteman (Eds.), *Snow and Ice-Related Hazards, Risks, and Disasters* (2nd ed., pp. 417–466). https://doi.org/10.1016/B978-0-12-817129-5.00003-2

Tsai, V. C., Smith, L. C., Gardner, A. S., & Seroussi, H. (2022). A unified model for transient subglacial water pressure and basal sliding. *Journal of Glaciology*, *68*(268), 390–400. https://doi.org/10.1017/jog.2021.103

Van Pelt, W. J. J., Oerlemans, J., Reijmer, C. H., Pohjola, V. A., Pettersson, R., & Van Angelen, J. H. (2012). Simulating melt, runoff and refreezing on Nordenskiöldbreen, Svalbard, using a coupled snow and energy balance model. *The Cryosphere*, *6*(3), 641–659. https://doi.org/10.5194/tc-6-641-2012

Zhan, Z. (2019). Seismic noise interferometry reveals transverse drainage configuration beneath the surging Bering Glacier. *Geophysical Research Letters*, *46*(9), 4747–4756. https://doi.org/10.1029/2019GL082411